Molina Puerto, J.; Oliveira, FR.; Souto, AP.; Esteves, MF.; Bonastre Cano, JA.; Cases Iborra, FJ. (2013). Enhanced adhesion of polypyrrole/PW12O403- hybrid coatings on polyester fabrics. Journal of Applied Polymer Science. 129(1):422-433. doi:10.1002/APP.38652.

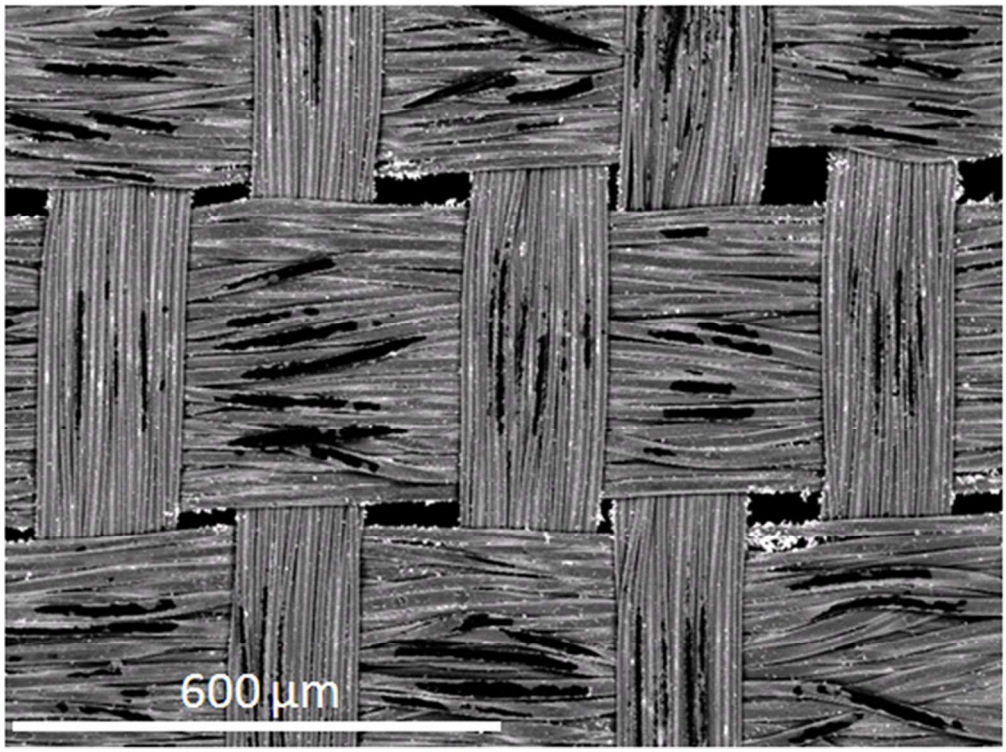

37x27mm (600 x 600 DPI)

Enhanced adhesion of polypyrrole/$PW_{12}O_{40}^{3-}$ hybrid coatings on polyester fabrics

J. Molina[a], F.R. Oliveira[b], A.P. Souto[b], M.F. Esteves[b], J. Bonastre[a], F. Cases[a,*]

[a]*Departamento de Ingeniería Textil y Papelera, EPS de Alcoy, Universitat Politècnica de València, Plaza Ferrándiz y Carbonell s/n, 03801 Alcoy, Spain*

[b]*Department of Textile Engineering, University of Minho, Campus de Azurém, 4800-058 Guimaraes, Portugal*

Abstract

Polyester fabrics have been treated with plasma to increase polypyrrole/$PW_{12}O_{40}^{3-}$ (hybrid material) adhesion to its surface. With the plasma treatment, the roughness of the fibers increases as it has been observed by means of atomic force microscopy (AFM). Polar functional groups are also created on the surface of polyester fabrics as X-ray photoelectron spectroscopy (XPS) measurements have shown. These polar groups contribute to the adhesion of polypyrrole to the fibers. Coatings obtained on plasma treated fabrics were more resistant to washing and rubbing fastness tests. The use of an inorganic counter ion ($PW_{12}O_{40}^{3-}$) that contains an element with a high atomic number (W) helps to locate zones where the coating is missed; this is achieved by means of micrographs obtained by backscattered electrons (BSE). The electrical resistance of the fabrics was also measured by electrochemical impedance spectroscopy (EIS), obtaining also better results with the plasma treated fabrics.

Keywords: plasma treatment, coatings, conducting polymers, polypyrrole, adhesion, electrochemistry.

* Corresponding author. Fax: +34 96 652 8438; telephone: +34 96 652 8412.

E-mail addresses: fjcases@txp.upv.es (Prof. F. Cases), javimolinetty@hotmail.com (Dr. J. Molina).

1. Introduction

The development of textiles with new properties and applications has received great attention during the last years; one of these properties is the electrical conductivity. One of the methods that have been employed to produce conducting fabrics is the chemical synthesis of polypyrrole on fabrics [1-9]. The chemical synthesis of polypyrrole on the fabrics produces a thin and continuous layer of conducting polymer that allows the electrical conduction in the fabrics. Applications of polypyrrole-based conducting fabrics are varied and numerous, such as antistatic materials [1], gas sensors [2], biomechanical sensors [3], electrotherapy [4,5], heating devices [6-8] or microwave attenuation [9].

One of the drawbacks of the chemical synthesis of polypyrrole on fabrics is the poor adhesion between the fibers and the polypyrrole coating. This makes that their mechanical properties are not as good as it would be desired. The polymerization of pyrrole is quite independent of the substrate. Only the polarity of the surface may have an effect on the adhesion of the conducting polymer. The adhesion is worse with fibers without polar groups (polyethylene for example) [10]. A way to improve the durability of the coating is to increase the surface energy of the fibers. Plasma treatments have

been proposed as an alternative to increase the adhesion between the fibers and the conducting polymer [11,12]. Plasma treatments have the advantage compared to chemical methods [13] that wastewaters are not generated [12]. Plasma treatment creates reactive groups and radicals on the surface of the fabric. In the present work we have employed polyester since it is a fiber widely employed in textile industry. Garg *et al.* studied the effect of glow discharge plasma on the adhesion of polypyrrole/AQSA (anthraquinone sulfonic acid) (organic counter ion) on polyester fabrics [12]. However, a study of functional groups generated and the change in the morphology of the fibers was not dealt. Plasma treatment can oxidize polyester surface breaking the ester bonds creating radicals [14]. These radicals can react with the plasma gas generated and create hydroxyl, carbonyl and carboxyl groups. These polars groups allow the formation of dipolar interactions, van der Waals forces or hydrogen bonds between the fabric and the coating, increasing the adhesion of the coating to the surface of the fabric [15]. Plasma treatments also modify the morphology of the fibers, creating a rougher surface that allows the creation of more contact points between the fiber and the coating (physical interaction). This could also improve the adhesion between coatings and the fibers [14]. There are different plasma methods available. In the present work we have employed dielectric barrier discharge (DBD). DBD is a type of cold plasma generated by an electric discharge in atmospheric conditions. Electric discharge takes place between two electrodes separated by a small gap where the fabric is continuously treated at a controlled speed. Fabric modification by plasma methods has the advantage that no water and other chemical products are needed. The low temperature achieved by DBD also allows little deterioration of organic samples [12].

During the synthesis of polypyrrole, positive charges are created in its structure (polarons and bipolarons). These positive charges are compensated by anions that act as

counter ions to maintain the electroneutrality principle. Typical counter ions employed in textiles coated with polypyrrole, are organic molecules with high size, such as: anthraquinone sulfonic acid (AQSA) [2,7,9,12,16-18], dodecylbenzene sulfonic acid (DBSA) [1,17], p-toluene sulfonic acid (PTSA) [2,9,17,19], naphthalenedisulfonic acid (NDSA) [3,9,17], benzenesulfonic acid (BSA) [4,20], naphthalenesulfonic acid (NSA) [9,19], anthraquinone disulfonic acid [21,22]. However, very little has been reported about the use of inorganic anions as counter ions when obtaining conducting fabrics. In our previous work [18], we employed an inorganic anion as counter ion ($PW_{12}O_{40}^{3-}$) to produce polypyrrole-based conducting fabrics. A hybrid organic/inorganic coating was obtained (PPy/$PW_{12}O_{40}^{3-}$). That paper was centered in the synthesis of PPy/$PW_{12}O_{40}^{3-}$ coatings in the optimal conditions and its characterization. In the present paper the employment of plasma treatments as a method to increase PPy/$PW_{12}O_{40}^{3-}$ adhesion has been performed and evaluated. The advantage of employing $PW_{12}O_{40}^{3-}$ as counter ion is that it presents an element with high atomic weight (W) in its structure. This allows obtaining micrographs with backscattered electrons (BSE) and makes it simpler to identify zones where the coating has been removed or damaged. Typical organic counter ions mentioned previously only have S (with low atomic weight) in its structure and only micrographs with secondary electrons (SE) are obtainable. With secondary electrons the contrast between the zones degraded and not degraded is worst and the evaluation of the degradation is more difficult. The previous study of Garg *et al.* [12] only evaluated the degradation of the coating by means of surface resistivity and a SEM study was not presented possibly due to this reason.

Polyester fabrics treated with different plasma dosages ($W \cdot min \cdot m^{-2}$) have been obtained. Static and dynamic contact angles have been measured to obtain the optimum plasma dosage. Atomic force microscopy (AFM) has been employed to observe surface

topography changes and obtain its roughness. X-ray photoelectron spectroscopy (XPS) measurements have been used to perform elemental analysis as well as to observe the formation of the different polar groups after plasma treatment. Fabrics untreated and treated with the optimum plasma dosage have been coated with polypyrrole/$PW_{12}O_{40}^{3-}$ and washing/rubbing fastness tests have been performed. Scanning electron microscopy (SEM) measurements have been employed for morphology observation and evaluation of the degradation of the coatings. Electrical resistance changes after rubbing fastness tests have been measured by electrochemical impedance spectroscopy (EIS).

Regarding the novelty of the topic, although plasma treatments have been employed previously for increasing conducting polymers adhesion on fabrics, a complete study of the functional groups generated during the plasma treatment and the change of the roughness has not been reported. Also the employment of an inorganic counter ion allows obtaining micrographs with backscattered electrons, helping to locate the zones were the coating was missed. With the traditional organic counter ions employed in bibliography it is difficult to locate these zones. Evidence of the degradation process has been also observed by SEM.

2. Experimental

2.1. Reagents and materials

Analytical grade pyrrole and ferric chloride were purchased from Merck. Normapur acetone was from Prolabo. Analytical grade phosphotungstic acid hydrate was supplied by Fluka. Ultrapure water was obtained from an Elix 3 Millipore-Milli-Q Advantage A10 system with a resistivity close to 18.2 MΩ cm. Commercial polyester fabrics with a warp density of 42 threads/cm, a weft density of 24 threads/cm and a surface density of

62 g m^{-2} were used in this study. These are specific terms used in the field of textile industry and their meaning can be consulted in a textile glossary [23].

2.2. Dielectric barrier discharge (DBD) treatment

Plasma treatment of polyester was carried out at atmospheric pressure with the dielectric barrier discharge modality (DBD) (Softal/University of Minho patented prototype) [24]. The equipment has a width of 50 cm and the following components: a metallic electrode coated with ceramic; a metallic counter electrode coated with silicone; an electric generator and a high tension transformer. The velocity (v) and power (P) are variable and the fabric passes through the electrodes continuously. The plasma dosage is defined by the equation (1) [24]:

$$dosage = \frac{N \cdot P}{v \cdot w} \qquad (1)$$

Where: N (number of passages), P (power, W), v (velocity, $m \bullet min^{-1}$), w (width, 0.5 m). For the treatment of polyester fabrics, velocity and power were maintained constant and the number of passages was varied. Table 1 shows the conditions employed for the treatments. The machine has a width of 50 cm so fabrics up to this width can be treated; several meters of fabric can be treated at a time. If larger quantities of fabric would be needed to be treated, rollers could be mounted on the machine. For example, to treat one meter long fabric with 4500 $W \bullet min \bullet m^{-2}$ (which was the optimal plasma dosage employed) with the velocity of 4 m/min, 0.25 min per passage would be needed. Since 9 passages were employed, the total treatment time would be 2.25 min per side of the fabric. So the total time to treat both sides of the fabric with 4500 $W \bullet min \bullet m^{-2}$ would be 4.5 min.

2.3. Contact angle measurements

Goniometer Dataphysics equipment using OCA software with video system for the caption of images in static and dynamic modes has been used for the measurement of contact angles of the water drops in untreated and plasma treated polyester fabrics. A drop of 5 µl of distilled water was put on the fabrics surface with a microliter syringe and observed with an especial CCD camera. At least five measurements at different places were taken for each fabric. The camera takes an image every 0.04 sec.

2.4. X-ray photoelectron spectroscopy measurements

XPS analyses were conducted at a base pressure of $5 \cdot 10^{-10}$ mbars and a temperature around -100 ºC. XPS spectra were obtained with a VG-Microtech Multilab electron spectrometer by using unmonochromatized Mg Kα (1253.6 eV) radiation from a twin anode source operating at 300 W (20 mA, 15 kV). The binding energy (BE) scale was calibrated with reference to the C1s line at 284.6 eV. C1s, O1s and N1s high resolution core level spectra were obtained and analyzed.

2.5. Morphological characterization of the fabrics

A Jeol JSM-6300 scanning electron microscope was employed to observe the morphology of the samples with and without DBD plasma treatment.

Atomic force microscopy (AFM) was used to determine surface topography and roughness of untreated and plasma treated samples. AFM analyses were performed with a multimode AFM microscope with a Nanoscope® IIIa ADCS controller (Veeco Metrology Group). A monolithic silicon cantilever (FESP, tip radius 8 nm, Bruker AFM probes) with a constant force of 2.8 N/m and a resonance frequency of 75 kHz was used to work on tapping mode. From the analysis of the images, the root-mean-squared

roughness (Rrms) measured on 500 nm x 500 nm images was evaluated. Section roughness was also evaluated.

2.6. Chemical synthesis of PPy/$PW_{12}O_{40}^{3-}$ on polyester fabrics

Chemical synthesis of PPy on polyester textiles was done as reported in our previous work [18]. The size of the samples was 12 cm × 6 cm approximately. Previously to reaction, polyester was degreased with acetone in an ultrasound bath and washed with water. Pyrrole concentration employed was 2 g/l and the molar relations of reagents employed in the chemical synthesis bath were pyrrole: $FeCl_3$: $H_3PW_{12}O_{40}$ (1: 2.5: 0.2). The next stage was the adsorption of pyrrole and counter ion ($PW_{12}O_{40}^{3-}$) (V = 500 ml) on the fabric for 30 min without stirring. At the end of this time, the $FeCl_3$ solution (V = 100 ml) was added and oxidation of the monomer took place during 150 min without stirring. Adsorption and reaction were performed in a precipitation beaker. The conducting fabric was washed with water to remove PPy not fixed to fibers and dried in a desiccator for at least 24 hr before measurements.

2.7. Washing and rubbing fastness tests

Washing and rubbing fastness tests were performed to quantify the resistance of polypyrrole coatings to physical actions. Washing tests were performed according to the ISO 105-C06-2010 norm. The method applied was the A1S (40 ºC, 30 min). A multifiber fabric made with the following fibers was employed; acetate (AC), cotton (CO), polyamide (PA), polyester (PES), polyacrylic (PAC) and wool (WO). Rubbing fastness tests of fabrics coated with polypyrrole were performed as explained in the norm ISO 105-X12:2001. Each sample was abraded against cotton abrasive fabric for 10 cycles. Color discharge for both tests was evaluated with a spectrophotometer

Datacolor Spectraflash SF 600 Plus CT for a D_{65} illuminant and an observer located at 10º in the 360-700 nm wavelength range. The relative color strength (K/S) values were calculated prior to carrying out the washing tests as a measurement of the quantity of polypyrrole deposited on the fabrics. The values were calculated employing the Kubelka-Munk equation (Eq. 2), where K and S stand for the light absorption and scattering, respectively, and R is the evaluated reflectance. Ten measurements were averaged for each sample analyzed.

$$K/S = \frac{(1-R)^2}{2R} \qquad (2)$$

Scanning electron microscopy (SEM) was also employed to observe the morphology of the samples coated with polypyrrole before and after rubbing fastness tests. All SEM measurements were performed using an acceleration voltage of 20 kV. Micrographs were obtained with secondary electrons (SE) and also with backscattered electrons (BSE). The presence of W allows obtaining micrographs employing BSE, in these micrographs the degradation of the coating can be easily observed as darker zones. Samples for SEM measurements were coated with Au employing a Sputter Coater Bal-Tec SCD 005. Samples to obtain micrographs employing BSE were coated with C to avoid the interference of Au.

2.8. Electrical measurements

An Autolab PGSTAT302 potentiostat/galvanostat was employed to perform electrochemical impedance spectroscopy (EIS) analyses. EIS measurements were performed in the 10^5-10^{-2} Hz frequency range. The amplitude of the sinusoidal voltage was ± 10 mV. Measurements were carried out in a two-electrode arrangement. In the configuration employed, the sample was located between two round copper electrodes (A = 1.5 cm^2).

3. Results and discussion

3.1. Contact angle measurements

The surface properties of polyester fabrics were analyzed by contact angle measurements to evaluate the effect of different plasma dosages and to choose the optimal dosage to apply.

The averaged advancing contact angle (θ) for untreated polyester was 87.6º, similar values have been observed in bibliography for untreated polyester [14,25,26]. After treating the fabric with a plasma dosage of 500 W•min•m^{-2}, the static contact angle decreased to 48.1º. This decrease continued with the increasing applied dosage (47.3º and 45º for 1500 and 3000 W•min•m^{-2}, respectively). With the treatment of 4500 W•min•m^{-2}, the contact angle decreased to 36.6º. A larger increase of the plasma dosage did not produce a significant decrease of the contact angle, with 6000 W•min•m^{-2} and 7500 W•min•m^{-2}, 34.4º and 32.1º were obtained, respectively. On the other hand, the energy consumption was increased, this is why 4500 W•min•m^{-2} was selected as the optimal plasma dosage. Surface energy can be calculated by different equations depending on the solvent or solvents employed to measure the contact angle [12,27]. Surface energy of the different samples was estimated according to the Young-Dupré equation [12]:

$$E = \gamma \cdot (1 + \cos(\theta)) \qquad (3)$$

Where: E is the surface energy (mJ/m^2), γ is the surface tension of water (72.8 mJ/m^2) and θ is the static contact angle in degrees. According to this equation the surface energies obtained were: 75.8 mJ/m^2 (polyester), 121.4 mJ/m^2 (PES + 500 W•min•m^{-2}), 122.2 mJ/m^2 (PES + 1500 W•min•m^{-2}), 124.3 mJ/m^2 (PES + 3000 W•min•m^{-2}), 131.2

mJ/m^2 (PES + 4500 W•min•m^{-2}), 132.9 mJ/m^2 (PES + 6000 W•min•m^{-2}) and 134.5 mJ/m^2 (PES + 7500 W•min•m^{-2}). The data obtained confirmed that the surface energy increased with the plasma dosage until it stabilized for 4500 W•min•m^{-2}.

These results suggest that the surface of the treated PES samples has been significantly changed due to the plasma treatment, which tends to create oxidized species on the surface of the polyester fibers (3.2 section). The roughness and microporosity of the fabrics is also increased as explained in AFM analyses (section 3.4). These variations produce an increase of the surface energy of the fabric, decreasing the contact angle and increasing their wettability [12].

The dynamic contact angle measurements can be used to study the effects of different plasma treatment on the fiber surface wettability [28]. Fig.1 shows the results obtained for the different polyester fabrics. The wettability of the fabric is highly improved by the plasma treatment. The contact angle (°) variation of the water drop (5 µl) along the time is highly dependent on the plasma dosage applied. As the drop contacts the surface it spreads, reaching the static contact angle (θ). Then the water drop starts to be absorbed by the fabric decreasing its volume steadily, and thus decreasing the contact angle until the total penetration is achieved. As can be observed in Fig. 1, a faster decrease of contact angle was observed for the PES samples treated with higher dosages (W•min•m^{-2}). Similar results have been reported in literature for different synthetic and natural fibers, mentioning modifications in accessible polar groups at the surface and creation of microporosity as the main reasons for this decrease [29-31]. With plasma activation it is possible to improve considerably the absorption velocity. This criterion was used to choose the optimal plasma dosage to be applied. According to the results obtained, the dosage of 4500 W•min•m^{-2} was employed as the optimal one to treat polyester fabrics. A higher increase of the plasma dosage did not produce an

improvement of the dynamic contact angle, the sample treated with 7500 $W \cdot min \cdot m^{-2}$ is also shown in Fig. 1. As it can be seen it is very similar to the obtained with 4500 $W \cdot min \cdot m^{-2}$, there was not an improvement.

3.2. X-ray photoelectron spectroscopy measurements

Fig. 2 a,b (C_{1s}), c,d (O_{1s}), e,f (N_{1s}) show the high resolution spectra for untreated (Fig. 2-a,c,e) and plasma treated polyester (Fig. 2-b,d,f). If we compare the high resolution C1s spectra for untreated an plasma treated polyester (Fig. 2-a,b) we can observe that the same peaks appear on both spectra. The three peaks are centered at 284.6, 286.2 and 288.5 eV. The first peak at 284.6 eV was attributed to C-C, C-H [32,33]. The second peak at 286.2 eV was assigned to C-O [32,33], and the third peak was attributed to O-C=O (ester) groups [32,33]. It could be observed that the latter band increased from 11 % to the 18.5 % after plasma treatment. Conversely, the band at 284.6 eV decreased (from 64 % to 58 %), indicating the oxidation of C-C and C-H by the DBD treatment. This clearly indicates the oxidation of the polyester surface produced by the plasma treatment. The oxidation is believed to be produced on C-C and C-H rather than on the ester groups of polyester [34].

Fig. 2-c,d show the high resolution O_{1s} spectra for untreated and plasma treated polyester. The same two peaks were observed for both samples. The first peak located around 531.9 eV was attributed to C=O groups and the second peak at 533.4 eV was assigned to C-O groups [35]. The same scale has been employed for both samples for better comparison. It can be easily appreciated that there is an increase in the O_{1s} signal in the plasma treated sample (Fig. 2-d) with respect to the untreated sample (Fig. 2-c). The increase in the oxygen content indicates that new oxygen-containing polar groups

are formed on the polyester surface. These polar groups are responsible for the increase in the hydrophilicity observed in section 3.1.

Fig. 2-e,f show the high resolution N_{1s} spectra for untreated and plasma treated polyester. In this case the change produced after the plasma treatment is clear. The same scale has been employed in Fig. 2-e,f for better comparison. Originally, untreated polyester sample showed little N content as can be seen in Fig. 2-e. The signal obtained in this case was in the level of the noise. In the inset figure it is shown the same figure in a magnified scale. After plasma treatment the N content was significantly increased and three peaks appeared at 400.0, 401.5 and 407 eV. The first band has been attributed to C=N and the second band has been assigned to C≡N or N-C-O [32]. The third band with the highest binding energy (407.0 eV) was ascribed to species containing directly oxidized nitrogen such as nitrates [33].

The superficial composition of polyester fabrics before and after plasma treatment was also quantified. Elemental composition (% atomic) and O/C and N/C ratios were obtained and compared for untreated and plasma treated samples (Table 2). If we compare the elemental composition of both samples it can be seen that C content diminishes from 72.5 to 63 %. This diminution is caused by the plasma treatment. Since it is an atmospheric process, O and N are incorporated in polyester structure creating polar groups. The diminution of C is accompanied by an increase in the O and N content. It can be seen that the O/C ratio increases from 0.37 to 0.54; this indicates the creation of functional groups containing O. The N/C ratio also increases from 0.004 to 0.043. These polar groups created in the structure of polyester allow the formation of a mixture of different interactions between the fabric and the coating; such as: dipolar interactions, van der Waals forces or hydrogen bonds; increasing the adhesion of the coating to the surface of the fabric [15]. The decrease in the contact angle and the

consequent increase in the wettability of the plasma treated fabrics can be also explained by the creation of these polar groups.

3.3. Scanning electron microscopy

Scanning electron microscopy was employed to evaluate the morphology of the different samples studied. Fig. 3-a,b show the micrographs of polyester fibers prior to the plasma treatment. The fibers are quite smooth and only some imperfections can only be observed on its surface. After treating the fabric with plasma (4500 $W \cdot min \cdot m^{-2}$), the morphology of the fiber was changed (Fig. 3-c,d). In these figures a granular morphology could be observed. Plasma treatment has caused the removal of some material from the surface of the fabric, increasing its roughness. To evaluate the roughness change that is in the order of nm [12] atomic force microscopy (AFM) was employed (section 3.4).

Polypyrrole was chemically deposited on the surface of the fabric as detailed in section 2.6. Samples of polyester and polyester treated with plasma (4500 $W \cdot min \cdot m^{-2}$) were coated with the hybrid organic/inorganic material $PPy/PW_{12}O_{40}^{3-}$. Fig. 3-e shows the sample of untreated polyester coated with $PPy/PW_{12}O_{40}^{3-}$. In this figure it can be seen that a continuous layer of the conducting polymer has been formed on the surface of the fibers. It is also noticeable the presence of globules of polypyrrole on the surface of the coating. This type of morphology is the typical observed in the formation polypyrrole coatings on fabrics [18]. The thickness of this coating has been estimated in our previous work to be about 400 nm [36]. Fig. 3-f shows the $PPy/PW_{12}O_{40}^{3-}$ coating on the surface of polyester treated with plasma (4500 $W \cdot min \cdot m^{-2}$). In this micrograph it can be also observed the formation of the coating. However, in this case besides the formation of small globules, the presence of polypyrrole in the form of spheres and in

the form of fibers can be pointed out (Fig. 3-f). This type of morphology has not been observed in untreated polyester as can be observed in Fig. 3-e.

3.4. Atomic force microscopy

Scanning electron microscopy (SEM) has not sufficient vertical resolution to appreciate variations of the topography at the nanometer scale and evaluate the roughness of the surface. For this reason, atomic force microscopy (AFM) measurements were employed. In addition, AFM has the advantage that no material is added to coat the samples [37]. In SEM, samples are coated with Au or C. AFM measurements were done to obtain the 3-D representation of the topography of the fibers (untreated and treated with DBD) and evaluate its variation as well as the roughness increase after plasma treatment [35,37-39]. DBD treatment causes the removal of part of the material increasing the surface roughness of the fibers. 3-D representations of 500 x 500 nm were obtained. Fig. 4-a,b compare the topography of polyester fiber before and after plasma treatment, respectively. The surface of the original fiber of polyester is quite smooth with no mentionable topographical features (Fig. 4-a). The root-mean-squared roughness (Rrms) obtained for this 3-D representation was 2.518 nm. However, after plasma etching, the appearance of valleys and summits can be seen in Fig. 4-b. After plasma treatment, Rrms increased till 7.624 nm. Fig. 4-c,d shows the 2-D representation of the same images shown in Fig. 4-a,b. In these images a section of the 3-D representation was obtained (white line) to evaluate its roughness. Fig. 4-e,f show the section roughness of untreated and plasma treated polyester, respectively. For untreated polyester fibers, Rrms obtained was 1.160 nm vs. 7.056 nm for the DBD treated fiber. The increase of the roughness allows a better physical interaction between the fabric and the coating and also produces a higher surface energy, decreasing the water drop

contact angle as it was explained in section 3.1. This increase in the surface energy would contribute to create a coating with better adhesion to the polyester surface.

3.5. Washing and rubbing fastness tests

Fig. 5 shows color strength (K/S) for untreated and plasma treated samples (both coated with PPy/$PW_{12}O_{40}^{3-}$), before and after washing tests. This figure shows that the color strength for the treated samples is higher than the untreated ones. The surface modification of the polyester substrate after DBD treatment permits to obtain more color intensity (K/S = 949) when compared with the untreated sample (K/S = 744). This means that the plasma treated samples contain more polypyrrole than the untreated fabrics. Plasma treatment increases the wettability and hidrophilicity of the fibers causing a better transport of reactants (such as oligomers) within the fabric. After performing the washing test, the color strength decreased for both samples due to the elimination of polypyrrole aggregates that were not firmly fixed on the surface of the fibers. Values of color strength after washing tests were also higher for plasma treated fabrics (764 vs. 575) indicating higher polypyrrole content.

Degradation of the coating after washing and rubbing fastness tests was evaluated by means of color staining with a spectrophotometer. Washing fastness tests showed values of 4-5 for color staining, indicating that the coating is resistant to the washing test. Values of 4-5 for color staining were obtained for all the fibers of the multifiber fabric (AC, CO, PA, PES, PAC and WO) (Table 3). This indicates that the part of polymer lost after washing tests (as observed in the decrease of K/S values) is not transferred to the multifiber fabric but it remains in solution. Rubbing fastness tests showed significant degradation of the coating with the loss of part of the conducting polymer. In the fabrics it could be distinguished the fraction of the sample that had been submitted to friction.

Values for color discharge of 2-3 and 3 were obtained for the treated and untreated samples. These values indicate a significant degradation of the polypyrrole layer. The higher values of color staining, 3, for untreated polyester indicate a lower staining of the conducting polymer. This can be explained by the lower quantity of polymer deposited on the untreated polyester fabric as it was proved by color strength (K/S) values obtained (949 with treatment and 744 without treatment), according to Fig. 5. SEM measurements were employed to observe better the degradation mechanism of the coating, and EIS measurements to quantify conductivity changes.

Scanning electron microscopy was employed to observe the degradation of PPy/$PW_{12}O_{40}^{3-}$ coatings after rubbing fastness tests. Fig. 6 shows different micrographs of the sample of untreated/treated polyester and coated with PPy/$PW_{12}O_{40}^{3-}$ after performing rubbing fastness tests. These micrographs were obtained with backscattered electrons (BSE). The removal of part of the coating due to the friction is better observed with micrographs obtained with BSE. W that is present in the counter ion employed ($PW_{12}O_{40}^{3-}$), is an element with high atomic weight and this allows obtaining micrographs with BSE. The zones where W is present, appear as brighter zones due to the fact that W atoms backscatter more electrons than low weight elements (such as S present in traditionally employed organic counter ions). The zones where the coating of PPy/$PW_{12}O_{40}^{3-}$ has been removed appear as black zones. This allows obtaining rapidly the counter ion distribution and consequently the removal of PPy/$PW_{12}O_{40}^{3-}$ after rubbing fastness tests can be easily detected. Fig. 6-a,b show micrographs of the sample of polyester without treatment and coated with PPy/$PW_{12}O_{40}^{3-}$ after rubbing fastness tests. Fig. 6-a shows a micrograph (x100) where the damage produced by friction can be easily observed. The PPy/$PW_{12}O_{40}^{3-}$ coating has been removed from the surface of several fibers. The damaged zones appear as black zones. These defects can be observed

better in Fig. 6-b where a micrograph with higher magnification is shown (x500). The mechanism of degradation seems to be a delamination process. The low adhesion between the polyester fiber and the PPy coating causes the formation of PPy sheets under the stress caused by the friction. Fig. 6-c,d show micrographs of the polyester fabric treated with plasma (4500 $W \cdot min \cdot m^{-2}$) and coated with PPy/$PW_{12}O_{40}^{3-}$ after rubbing fastness tests. In Fig. 6-c it can be seen that the damage produced by the friction is lower than in the fabric without plasma treatment (Fig. 6-a). Only some black spots indicating coating removal can be detected. This can be clearly observed if we compare Fig. 6-a and Fig. 6-c. The zones affected by friction are lower in the case of plasma treated polyester since only the formation of few defects can be observed. These defects are also smaller than in the case without plasma treatment. This can be observed in Fig. 6-d where a micrograph with higher magnification is shown, only three defects on the bottom of the micrograph can be observed. These results indicate that plasma treatment actually increases polypyrrole adhesion to the surface of polyester.

Fig. 7 shows different micrographs of the plasma treated (Fig. 7-a,b,c) and untreated samples (Fig. 7-d) and coated with PPy/$PW_{12}O_{40}^{3-}$. In this case micrographs were obtained with secondary electrons (SE). Fig. 7-a, shows a micrograph of a fiber of polyester treated with plasma and coated with PPy/$PW_{12}O_{40}^{3-}$ in a zone without friction. The surface of the fiber is coated with a continuous layer of PPy/$PW_{12}O_{40}^{3-}$; the presence of PPy globules on its surface is also noticeable. Fig. 7-b shows a micrograph of a fiber treated with plasma and coated with PPy/$PW_{12}O_{40}^{3-}$ in a zone with friction. It can be seen that the PPy coating has not been removed. In this case the degradation only takes place on the surface of the coating; PPy globules and part of the outermost coating have been removed by the friction. Fig. 7-c shows the same fiber in a zone where the coating has been removed and a defect has been formed. It can be seen that it is a

punctual defect and the coating has been only removed in this part, there is no delamination process affecting the surrounding coating. On the other hand, in the fiber without treatment (Fig. 7-d) it can be seen that the coating is delaminated from the fiber surface, the delaminated PPy sheets can be clearly observed in this micrograph. The adhesion after plasma treatment increases and this avoids the removal of the coating by delamination processes; as it happened in the case of polyester without treatment. After plasma treatment, only punctual defects are formed and the degradation process only takes place on the outermost part of the coating.

3.6. Electrical measurements

Fig. 8 shows the Bode diagrams for the samples of PES, PES untreated + PPy/$PW_{12}O_{40}^{3-}$ before and after rubbing fastness tests, PES treated with plasma (4500 $W \cdot min \cdot m^{-2}$) + PPy/$PW_{12}O_{40}^{3-}$ before and after rubbing fastness tests. The data shown in these graphics were measured with the configuration where the sample was located between two round copper electrodes. In Fig. 8-a, it can be seen the impedance modulus (|**Z**|) at the different frequencies for the different samples. The sample of polyester presents a value of the impedance modulus at low frequencies higher than 10^{11} Ω, typical value of insulating materials. When the sample of polyester was coated with PPy/$PW_{12}O_{40}^{3-}$, the value of the impedance modulus lowered more than nine orders of magnitude. Untreated polyester coated with PPy/$PW_{12}O_{40}^{3-}$ showed values of the impedance modulus around 25 Ω; after rubbing tests the value was 50 Ω. The resistance of plasma treated polyester after applying the coating was 17 Ω and 24 Ω after the rubbing fastness test. Values of resistance can be better observed in Fig. 8-b. With the plasma treated polyester, the resistance obtained is lower since more polypyrrole has been deposited as color strength (K/S) values showed (section 3.5). After rubbing

fastness tests, the increase of resistance was also lower in plasma treated samples. Plasma treatment causes an increase of the adhesion and less polymer mass is lost after the rubbing fastness test as it has been observed by SEM. Consequently, the increase of the resistance is lower in the case of plasma treated polyester. One could expect higher loss of electrical conductivity when observing the degradation produced in the untreated samples (Fig. 6-a,b). However the degradation is only produced in the uppermost part of the fiber as we could see in the micrographs. The other parts of the fibers are still coated with PPy/$PW_{12}O_{40}^{3-}$ and this allows the electrical conduction, although an increase of the resistance is produced due to the lower area of conducting polymer remaining. Regarding applications, these fabrics can be employed as antistatic materials, since static charging of the surface of fibers is excluded with surface resistivity below 5×10^{9} Ω/ [40]. The values obtained were some orders of magnitude lower to the necessary one [41].

In Fig. 8-c, it is shown the data for the phase angle at different frequencies for the same samples of the first diagram. Polyester has a phase angle of nearly 90º, the data at low frequencies is not shown since noise due to the large values of impedance modulus was observed. This value of phase angle is typical of insulating materials that act as a capacitor. All PES-PPy/$PW_{12}O_{40}^{3-}$ conducting fabrics before and after rubbing fastness tests have shown 0º of phase angle in the entire frequency range. This indicates that the samples acted as a resistor (conducting material) with the different resistances that were indicated previously. So polyester changed its behavior from an insulating material to a conductor one after polypyrrole deposition.

4. Conclusions

Polyester fabrics have been treated with a plasma technique (dielectric barrier discharge) to modify its surface in order to increase the adhesion of polypyrrole/$PW_{12}O_{40}^{3-}$ hybrid coatings. Plasma modification causes the decrease of the contact angle (static and dynamic) and an increase of the wettability due to an increase of the surface energy of the fibers. These modifications are caused by the appearance of functional polar groups containing O and N, as XPS measurements have shown. In addition to this, the roughness of the fabric also is increased as atomic force microscopy (AFM) measurements have shown. Due to this fact, physical interaction between the fabric and the coating is increased, improving the mechanical adhesion. The durability of PPy/$PW_{12}O_{40}^{3-}$ coatings has been evaluated by means of washing and rubbing fastness tests. Washing tests have shown no significant degradation of the coating. However, rubbing fastness tests, which are more aggressive, produced the loss of part of the coating. In the case of untreated polyester, the degradation mechanism is a delamination process, due to the low adhesion between the fiber and the coating. Micrographs obtained by secondary electrons (SE) and backscattered ones (BSE) have shown this fact. In the case of plasma treated polyester, the degradation is caused by the friction of the outermost part of the coating. In this case, the coating is better adhered to the surface of the fiber due to the formation of a mixture of physical and chemical interactions (dipolar interactions, van der Waals forces and hydrogen bonds) and only part of the coating is lost. The presence of W in the counter ion ($PW_{12}O_{40}^{3-}$) was an advantage that allowed obtaining micrographs by backscattered electrons and observing easily the zones where the coating was removed. Friction caused an increase of the electrical resistance of the samples due to the formation of defects as it was measured by electrochemical impedance spectroscopy. This increase was lower in the case of plasma treated polyester due to a lower degradation of the coating since it was more

adhered to the surface of the fibers. The values of resistance obtained indicate that conducting fabrics can be used as antistatic materials.

Acknowledgements

Authors thank to the Spanish Ministerio de Ciencia e Innovación (contracts CTM2010-18842-C02-02 and CTM2011-23583) and Universitat Politècnica de València (Primeros Proyectos de Investigación (PAID-06-10)) for the financial support. J. Molina is grateful to the Conselleria d'Educació (Generalitat Valenciana) for the FPI fellowship.

Contribution of every listed author

J. Molina performed the synthesis of the materials and wrote the paper; F. R. Oliveira, A.P. Souto and M.F. Esteves performed the plasma treatment of the fabrics and its characterization by contact angle measurements and they also wrote this part of the paper. J. Bonastre performed the XPS measurements and analysis. F. Cases designed the experiments and wrote the paper.

References

[1] Lekpittaya, P.; Yanumet, N.; Grady, B. P.; O'Rear, E. A. *J. Appl. Polym. Sci.* **2004**, *92*, 2629–2636.

[2] Kincal, D.; Kumar, A.; Child, A; Reynolds, J. *Synth. Met.* **1998**, *92*, 53–56.

[3] Wu, J.; Zhou, D.; Too, C. O.; Wallace, G. G. *Synth. Met.* **2005**, *155*, 698–701.

[4] Oh, K. W.; Park, H. J.; Kim, S. H. *J. Appl. Polym. Sci.* **2003**, *88*, 1225–1229.

[5] Kim, S. H.; Oh, K. W.; Bahk, J. H. *J. Appl. Polym. Sci.* **2004**, *91*, 4064–4071.

[6] Bhat, N. V.; Seshadri, D. T.; Nate, M. N.; Gore, A. V. *J. Appl. Polym. Sci.* **2006**, *102*, 4690–4695.

[7] Hakansson, E.; Kaynak, A.; Lin, T.; Nahavandi, S.; Jones, T.; Hu, E. *Synth. Met.* **2004**, *144*, 21–28.

[8] Boutrois, J. P.; Jolly, R.; Pétrescu, C. *Synth. Met.* **1997**, *85*, 1405–1406.

[9] Kuhn, H.; Child, A.; Kimbrell, W. *Synth. Met.* **1995**, *71*, 2139–2142.

[10] Kuhn, H. H.; Child, A. D. In Handbook of Conducting Polymers; Skotheim, T. A.; Elsenbaumer, R. L.; Reynolds, J. R., Eds.; Marcel Dekker, Inc.: New York, **1998**, Chapter 19, pp 993-1013.

[11] Oh, K. W.; Kim, S. H.; Kim, E. A. *J. Appl. Polym. Sci.* **2001**, *81*, 684–694.

[12] Garg, S.; Hurren, C.; Kaynak, A. *Synth. Met.* **2007**, *157*, 41–47.

[13] Lin, S. P.; Han, J. L.; Yeh, J. T.; Chang, F. C.; Hsieh, K. H. *J. Appl. Polym. Sci.* **2007**, *104*, 655–665.

[14] Leroux, F.; Campagne, C.; Perwuelz, A.; Gengembre, L. *Surf. Coat. Technol.* **2009**, *203*, 3178–3183.

[15] Kan, C. W.; Chan, K.; Yuen, C. W. M.; Miao, M. H. *J. Mater. Process. Technol.* **1998**, *82*, 122-126.

[16] Lin, T.; Wang, L.; Wang, X.; Kaynak, A. *Thin Solid Films* **2005**, *479*, 77–82.

[17] Ferrero, F.; Napoli, L.; Tonin, C.; Varesano, A. *J. Appl. Polym. Sci.* **2006**, *102,* 4121–4126.

[18] Molina, J.; del Río, A. I.; Bonastre, J.; Cases, F. *Eur. Polym. J.* **2008**, *44*, 2087–2098.

[19] Lee, H. S.; Hong, J. *Synth. Met.* **2000**, *113*, 115–119.

[20] Gasana, E.; Westbroek, P.; Hakuzimana, J.; De Clerck, K.; Priniotakis, G.; Kiekens, P.; Tseles, D. *Surf. Coat. Technol.* **2006**, *201*, 3547–3551.

[21] Dall'Acqua, L.; Tonin, C.; Varesano, A.; Canetti, M.; Porzio, W.; Catellani, M. *Synth. Met.* **2006**, *156*, 379–386.

[22] Dall'Acqua, L.; Tonin, C.; Peila, R.; Ferrero, F.; Catellani, M. *Synth. Met.* **2004**, *146*, 213–221.

[23] Complete textile glossary. http://www.celaneseacetate.com/textile_glossary_filament_acetate.pdf (accessed June 10, 2012).

[24] Carneiro, N.; Souto, A. P.; Forster, F.; Prinz, E. Patent in internationalization phase (2004) /patent number PCT/PT2004/000008 (2004).

[25] Cioffi, M. O. H.; Voorwald, H. J. C.; Mota, R. P. *Mater. Charact.* **2003**, *50*, 209–215.

[26] Morent, R.; De Geyter, N.; Verschuren, J.; De Clerck, K.: Kiekens, P.; Leys, C. *Surf. Coat. Technol.* **2008**, *202*, 3427–3449.

[27] Ran, F.; Nie, S.; Zhao, W.; Li, J.; Su, B.; Sun, S.; Zhao C. *Acta Biomater.* **2011**, *7*, 3370–3381.

[28] Oliveira, F. R.; Souto, A. P.; Carneiro, N.; Nascimento, J. H. O. *Mater. Sci. Forum* **2009**, *636-637*, 846–852.

[29] Yip, J.; Chan, K.; Sin, K. M.; Lau, K. S. *Color. Technol.* **2002**, *118*, 26–30.

[30] Jia, C.; Chen, P.; Li, B.; Wang, Q.; Lu, C.; Yu, Q. *Surf. Coat. Technol.* **2010**, *204*, 3668–3675.

[31] Wielen, L. C. V.; Östenson, M.; Gatenholm, P.; Ragauskas, A. J. *Carbohyd. Polym.* **2006**, *65*, 179–184.

[32] Wilson, D. J.; Williams, R. L.; Pond, R. C. *Surf. Interface Anal.* **2001**, *31*, 385–396.

[33] Lynch, J. B.; Spence, P. D.; Baker, D. E.; Postlethwaite, T. A. *J. Appl. Polym. Sci.* **1999**, *71*, 319–331.

[34] De Geyter, N.; Morent, R.; Leys, C. *Surf. Coat. Technol.* **2006**, *201*, 2460–2466.

[35] Feng, J.; Wen, G.; Huang, W.; Kang, E. T.; Neoh, K. G. *Polym. Degrad. Stab.* **2006**, *91*, 12–20.

[36] Romero, E.; Molina, J.; del Río, A. I.; Bonastre, J.; Cases, F. *Text. Res. J.* **2011**, *81*, 1427–1437.

[37] Brzeziński, S.; Tracz, A.; Połowiński, S.; Kowalczyk, D. *J. Appl. Polym. Sci.* **2010**, *116*, 3659–3667.

[38] Švorčík, V.; Kolářová, K.; Slepička, P.; Macková, A.; Novotná, M.; Hnatowicz, V. *Polym. Degrad. Stab.* **2006**, *91*, 1219–1225.

[39] Sanchis, M. R.; Blanes, V.; Blanes, M.; Garcia, D.; Balart, R. *Eur. Polym. J.* **2006**, *42*, 1558–1568.

[40] Textor, T.; Mahltig, B. *Appl. Surf. Sci.* **2010**, *256*, 1668–1674.

[41] Molina, J.; Fernández, J.; del Río, A. I.; Bonastre, J.; Cases, F. *Appl. Surf. Sci.* **2011**, *257*, 10056–10064.

Figure captions

Fig. 1. Dynamic contact angle (°) measurements for polyester fabrics treated with different plasma dosages.

Fig. 2. C_{1s} (a,b), O_{1s} (c, d) and N_{1s} (e, f) XPS high resolution spectra for untreated (a, c, e) and plasma treated polyester (b, d, f).

Fig. 3. SEM micrographs of: a) PES without treatment (x10000), b) PES without treatment (x20000), c) PES treated 4500 $W \cdot min \cdot m^{-2}$ (x10000), d) PES treated 4500 $W \cdot min \cdot m^{-2}$ (x20000), e) PES without treatment + $PPy/PW_{12}O_{40}^{3-}$ (x2000), f) PES treated 4500 $W \cdot min \cdot m^{-2}$ + $PPy/PW_{12}O_{40}^{3-}$ (x1500).

Fig. 4. AFM 3D topographic representations of untreated a) and plasma treated polyester (4500 $W \cdot min \cdot m^{-2}$) b). AFM 2D roughness profiles of untreated c) and treated polyester d). Section roughness profile of untreated e) and treated polyester f).

Fig. 5. Color strength (K/S) for untreated and treated (4500 $W \cdot min \cdot m^{-2}$) PES samples coated with $PPy/PW_{12}O_{40}^{3-}$. Measurements done before and after washing tests.

Fig. 6. SEM micrographs obtained with backscattered electrons (BSE) of: PES without treatment + $PPy/PW_{12}O_{40}^{3-}$ after rubbing test; a) (x100), b) (x500). PES with plasma treatment (4500 $W \cdot min \cdot m^{-2}$) + $PPy/PW_{12}O_{40}^{3-}$ after rubbing fastness test; c) (x100), d) (x500).

Fig. 7. SEM micrographs obtained with secondary electrons (SE) of: PES with plasma treatment (4500 $W \cdot min \cdot m^{-2}$) + $PPy/PW_{12}O_{40}^{3-}$ after rubbing fastness test; a) (x5000), b) (x5000), c (x5000). PES without treatment + $PPy/PW_{12}O_{40}^{3-}$ after rubbing fastness test; d) (x5000).

Fig. 8. Bode plots for PES, untreated/treated PES + PPy/$PW_{12}O_{40}^{3-}$ before and after rubbing fastness tests. Sample located between two copper electrodes. Frequency range from 10^{5} Hz to 10^{-2} Hz.

Table captions

Table 1. Conditions and plasma dosages applied to polyester fabrics.

Table 2. Elemental composition (% atomic) and O/C and N/C ratios for untreated and plasma treated polyester (4500 W min m^{-2}).

Table 3. Values of color discharge of samples of polyester (untreated and treated with plasma) coated with PPy/$PW_{12}O_{40}^{3-}$ after washing fastness tests on different fabrics.

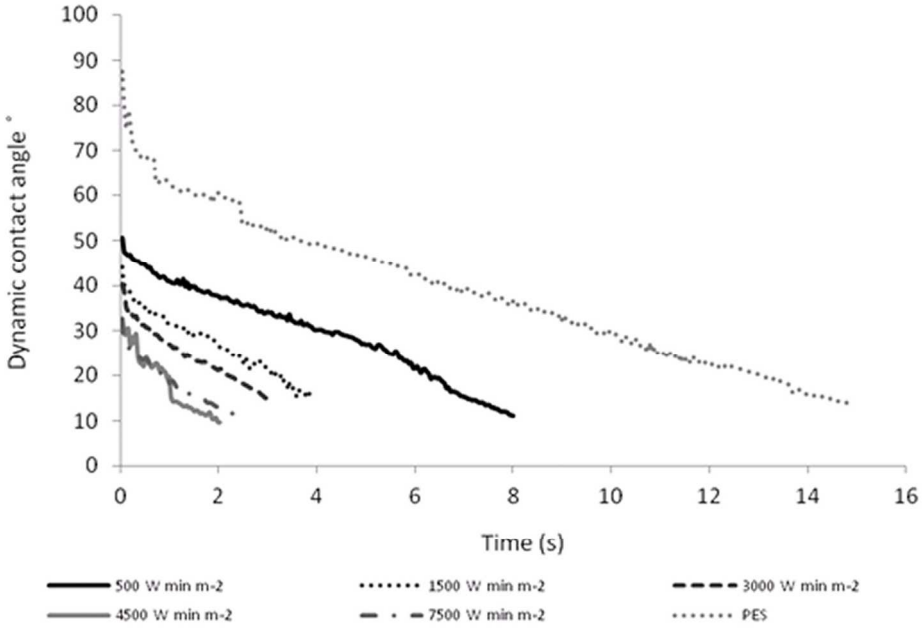

Fig. 1. Dynamic contact angle (°) measurements for polyester fabrics treated with different plasma dosages.
77x50mm (600 x 600 DPI)

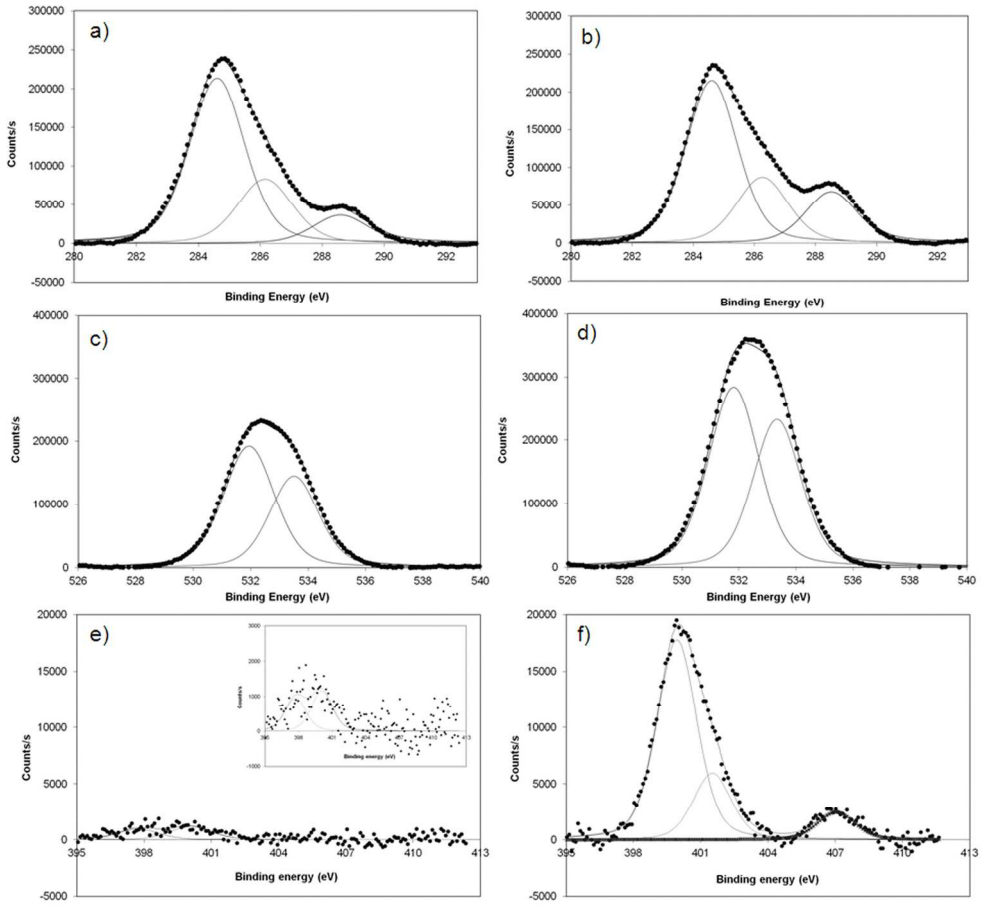

Fig. 2. C1s (a,b), O1s (c, d) and N1s (e, f) XPS high resolution spectra for untreated (a, c, e) and plasma treated polyester (b, d, f).
108x98mm (600 x 600 DPI)

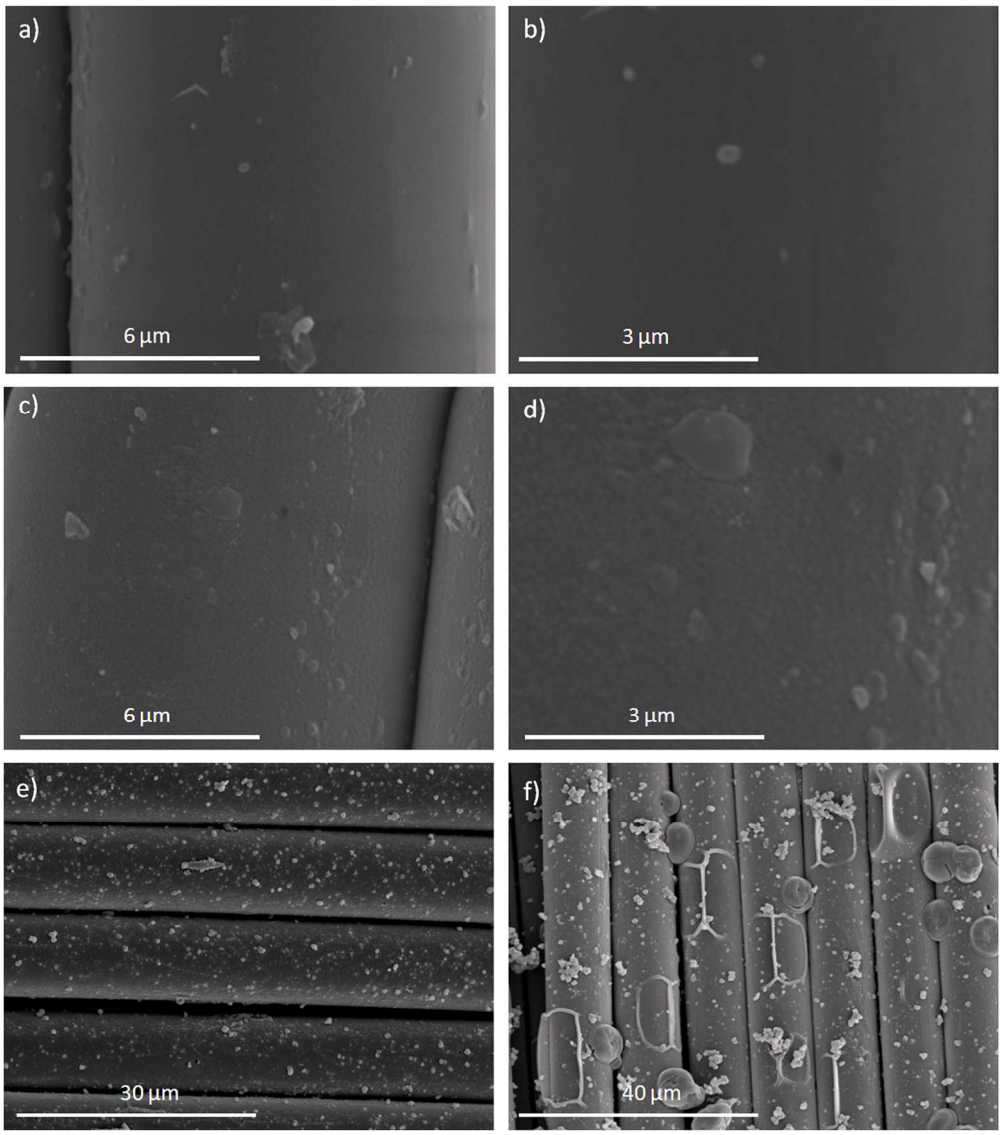

Fig. 3. SEM micrographs of: a) PES without treatment (x10000), b) PES without treatment (x20000), c) PES treated 4500 W min m-2 (x10000), d) PES treated 4500 W min m-2 (x20000), e) PES without treatment + PPy/PW12O403- (x2000), f) PES treated 4500 W min m-2 + PPy/PW12O403- (x1500).
135x152mm (600 x 600 DPI)

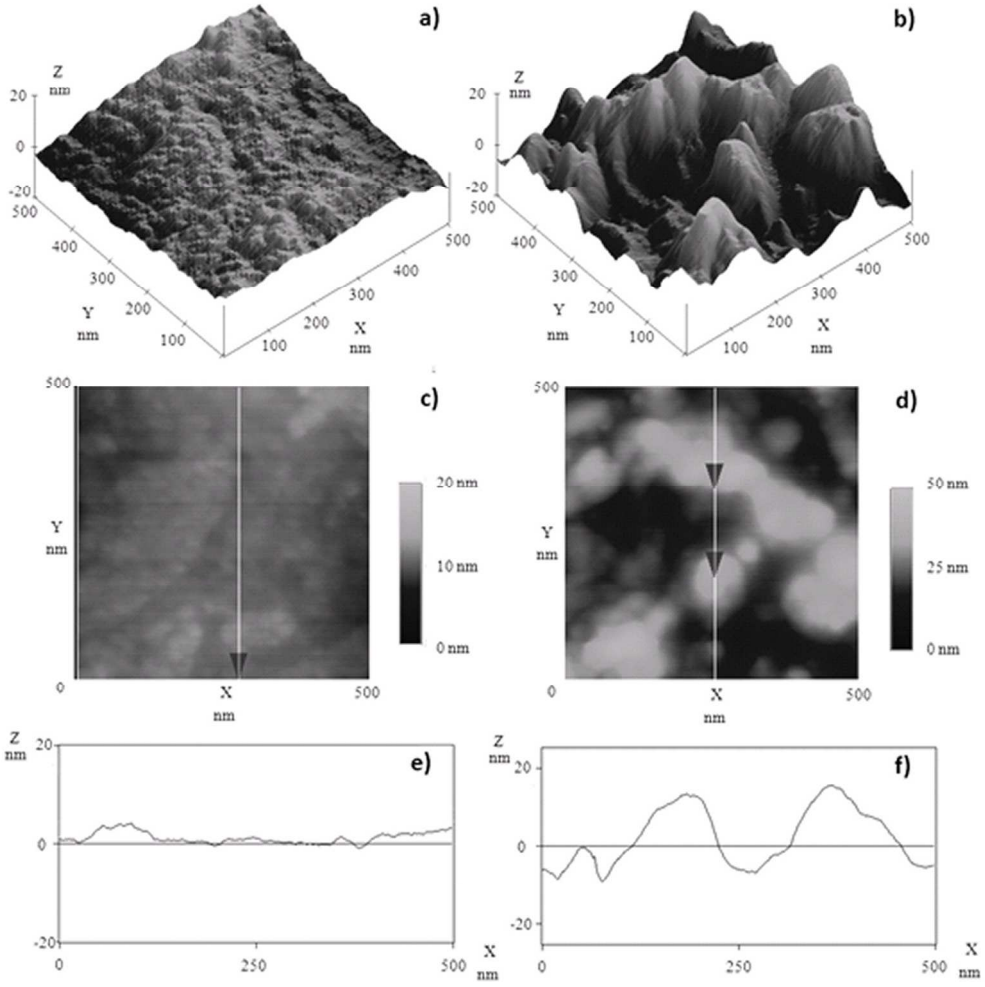

Fig. 4. AFM 3D topographic representations of untreated a) and plasma treated polyester (4500 W min m-2) b). AFM 2D roughness profiles of untreated c) and treated polyester d). Section roughness profile of untreated e) and treated polyester f).
119x118mm (600 x 600 DPI)

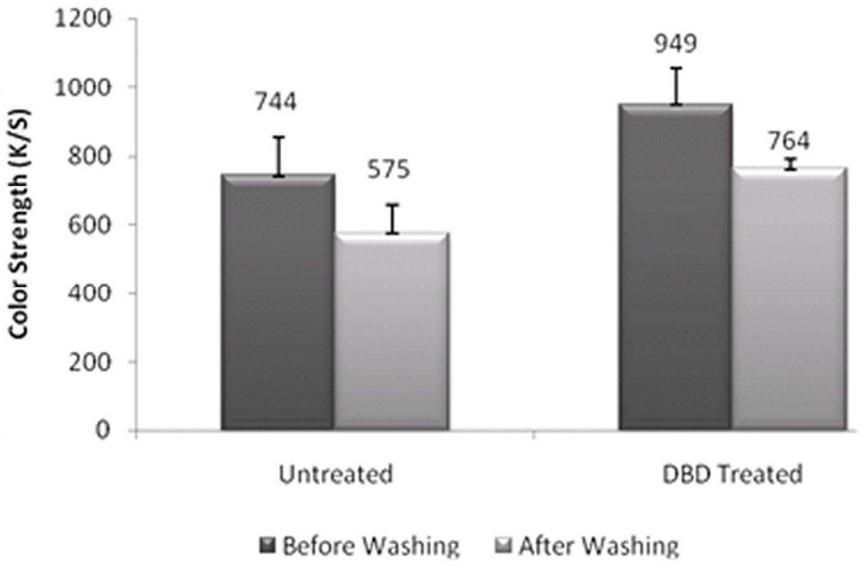

Fig. 5. Color strength (K/S) for untreated and treated (4500 W min m-2) PES samples coated with PPy/PW12O403-. Measurements done before and after washing tests.
72x43mm (600 x 600 DPI)

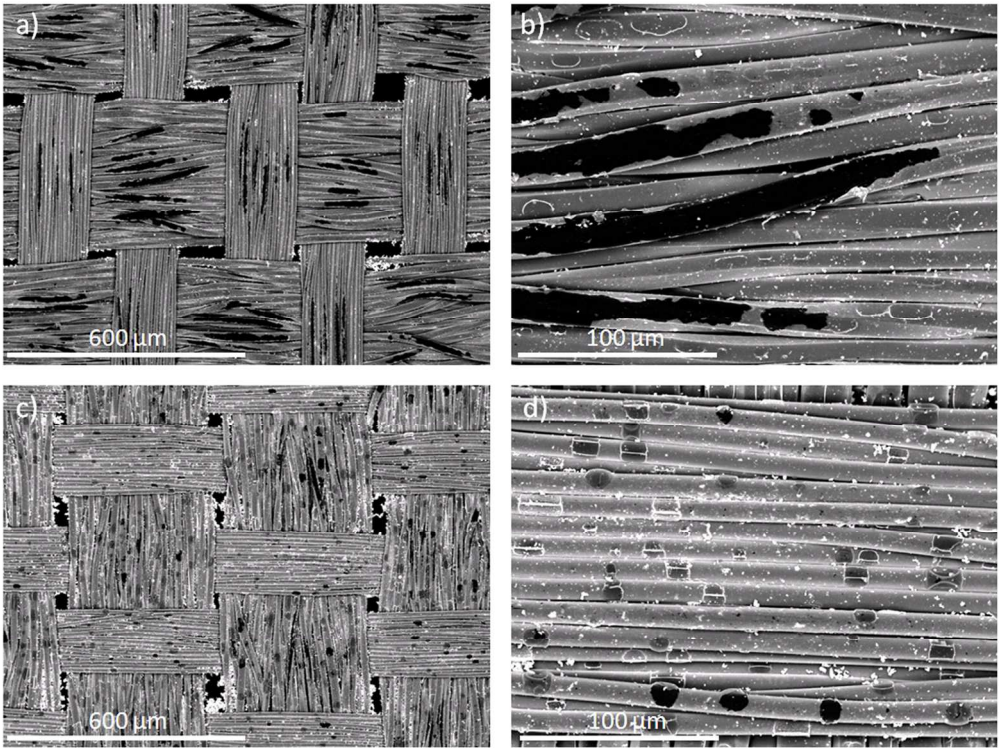

Fig. 6. SEM micrographs obtained with backscattered electrons (BSE) of: PES without treatment + PPy/PW12O403- after rubbing test; a) (x100), b) (x500). PES with plasma treatment (4500 W min m-2) + PPy/PW12O403- after rubbing fastness test; c) (x100), d) (x500).
90x67mm (600 x 600 DPI)

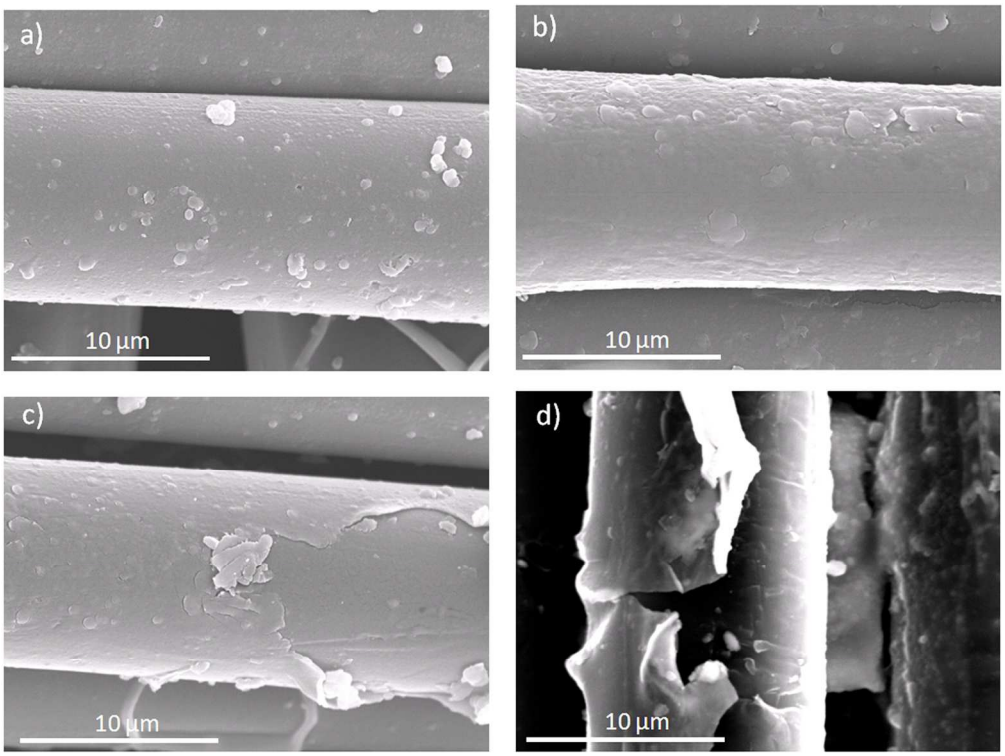

Fig. 7. SEM micrographs obtained with secondary electrons (SE) of: PES with plasma treatment (4500 W min m-2) + PPy/PW12O403- after rubbing fastness test; a) (x5000), b) (x5000), c (x5000). PES without treatment + PPy/PW12O403- after rubbing fastness test; d) (x5000).
90x68mm (600 x 600 DPI)

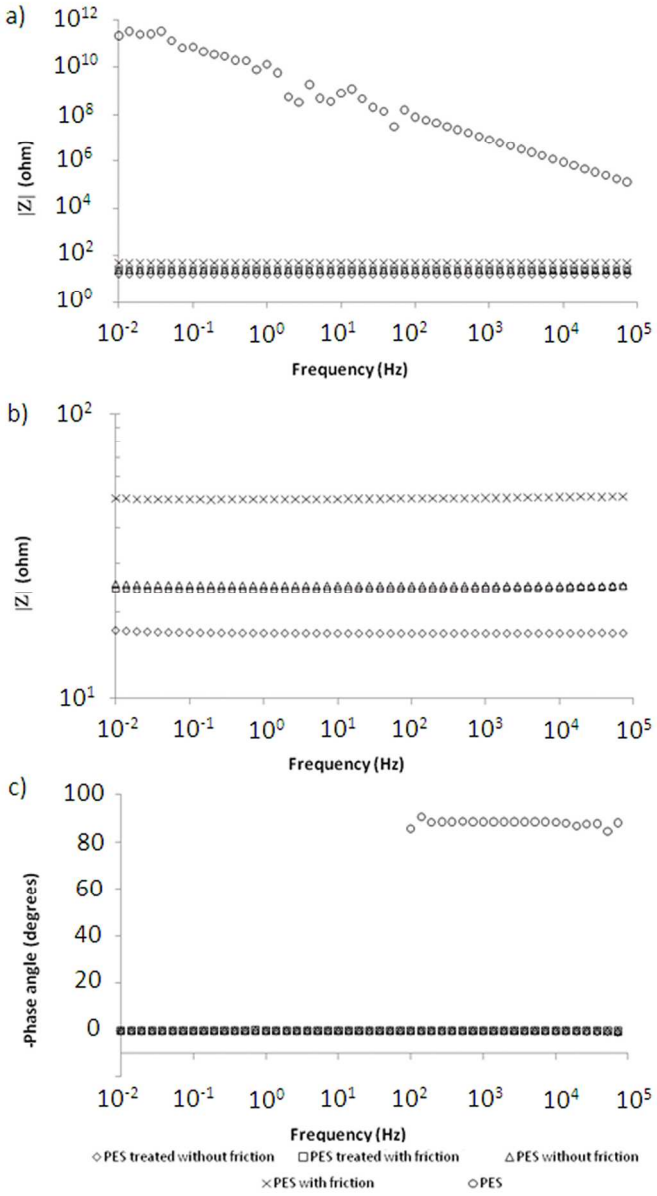

Fig. 8. Bode plots for PES, untreated/treated PES + PPy/PW12O403- prior and after rubbing fastness tests. Sample located between two copper electrodes. Frequency range from 105 Hz to 10-2 Hz.
213x380mm (600 x 600 DPI)

Sample	Velocity ($m \cdot min^{-1}$)	Power (W)	Number of passages	Dosage ($W \cdot min \cdot m^{-2}$)
1	4	1000	1	500
2	4	1000	3	1500
3	4	1000	6	3000
4	4	1000	9	4500
5	4	1000	12	6000
6	4	1000	15	7500

	% atomic			ratios	
Sample	C1s	O1s	N1s	O/C	N/C
Untreated PES	72.53	27.19	0.29	0.37	0.004
Plasma treated PES	63.09	34.17	2.74	0.54	0.043

Samples	AC	CO	PA	PES	PAC	WO
Untreated polyester	4/5	4/5	4	4	4/5	4/5
Treated polyester (4500 W·min·m^{-2})	4/5	4/5	4/5	4	4	4/5